Discrete Gust Response of a Box-wing Configuration

Rauno Cavallaro
University Carlos III of Madrid
Assistant Professor
Av. de la Universidad 30, 28911 Leganés , MA
Rauno.cavallaro@uc3m.es

Juan Palacios Santos
University Carlos III of Madrid
Undergraduate student

Rocco Bombardieri
University Carlos III of Madrid
PhD Candidate

ABSTRACT

This paper investigates the discrete symmetric gust response of an unconventional aircraft layout called Box Wing, also known as PrandtlPlane, and gives a very introductory perspective on the gust-induced stress states, and thus, insight into the structural design of such configuration. The typical box-wing aircraft features a closed-wing system that, seen frontally, reminds of a box shape. Its aerodynamics is characterized by mutual wing down/upwash interference and, from the structural point of view, it is an overconstrained system; these properties, as underlined by different studies, strongly complicate the design promoting counterintuitive behaviours. Regulations regarding symmetric gust response for the specific class of the aircraft are followed to set the gust parameters. With the aid of DYNRESP code, a robust tool for determining dynamic loads, the dynamic response of the flexible free-free aircraft is obtained for several gust parameters and two points in the envelope. The time-response is then critically analyzed, and also, based on the deformed shapes, few conditions are selected for a deeper investigation. Stress analyses performed on the chosen response instants showed that only marginal areas of the structure undergo higher stresses than those observed on the reference limit load (load factor 2.5) condition.

KEYWORDS: Box Wing, *Discrete Gust Response, PrandtlPlane, Aeroelasticity, Dynamic loads.*

NOMENCLATURE

B – Finite element damping matrix
B_{hh}- Generalized damping matrix
CoG – Center of Mass
F_A- Aerodynamic forces
F_g - Gust profile alleviation factor
H- Gust gradient
$h_{cr/sl}$ - Cruise/Sea level altitude
K- Finite element stiffness matrix
K_{hh}- Generalized stiffness matrix
M - Mach number
M - Finite element mass matrix
M_{hh}- Generalized mass matrix
n_z- load factor
q_∞- Dynamic pressure
Q_{hg}- Generalized gust force vector
Q_{hh}- Generalized aerodynamic matrix
s - Distance penetrated into the gust
t - Time
U_{ds} - Design gust velocity
U_{ref} - Reference gust velocity
V_c - Design cruise speed
W_g- Gust vertical velocity
ξ - Modal displacements
ϕ – Normal modes
ω - Frequency

1 INTRODUCTION

Last decades have witnessed a growing interest towards unconventional aircraft configurations. With an expected consistent growth of the passenger traffic and an increased attention towards sustainable aeronautics, ambitious goals have been set by the community leading entities.
In order to achieve such goals, several experts have supported the design of aircraft featuring different-than-conventional layouts. Among these novel configurations, the so called Box Wing, also known as PrandtlPlane [1], is currently considered as a viable option. The ongoing project **Parsifal** (Prandtlplane ARchitecture for the Sustainable Improvement of Future AirpLanes) financed by EU within the Horizon 2020 framework, demonstrates the attention of the community to the potentials of this configuration.
Box Wings feature a lifting system composed of two wings, placed at different heights, staggered, and interconnected at their wing-tip through a vertical joint. Looking at such lifting system frontally, the typical box shape is found, hence the name Box Wing. A pictorial view of the configuration is given in Fig. 1. According to Prandtl [2], such an arrangement provides the best performance in terms of induced drag, for a fixed wingspan and lift.
One of the first studies of an aircraft employing such lifting system dates back to the seventies, when Lockheed Martin performed a box-wing aircraft synthesis [3]. Results were noteworthy, however, flutter well inside the flight envelope was found and the lack of viable solutions to fix the issue made the studies on this configuration be discontinued.
Later on, Prof. Frediani's research group studied more in depth several aspects of the configuration [4]: its work spanned the last two decades and gave a deeper insight into the potentials of this layout; it also led to the manufacturing a full-scale prototype of a PrandtlPlane amphibious aircraft [5].
Among the studies carried out in the literature on Box Wings, relevant to this effort is [6] in which a structural design complying with multidisciplinary constraints was performed; the design was then further refined in [7], and use of composite materials as opposed to metallic ones was explored.
From a dynamic aeroelastic point of view, major contributions were given by efforts [8] first, and later on [9] [10] [11]; in particular, flutter properties were first investigated on a cantilever model, and it was later noted how inertial properties of the fuselage might increase the flutter speed. Not all the aspects regarding dynamic aeroelastic properties of the Box Wing were, however, studied.
Gust response of such configuration, for example, has never been investigated before.

Figure 1: Artistic view of the studied Box Wing (PrandtlPlane), rearranged from [13].

1.1 Contributions of the present study

The purpose of this paper is twofold.
First, and for the first time, the aeroelastic response to discrete symmetric gust will be carried out on a mid-size 250-seat PrandtlPlane. The process will follow the regulation specifications for discrete gust

design. The typical arrangement of the aerodynamic surfaces, as well as the structural response of the two wings connected through the joint into an overconstrained system, makes this problem unique, and far from trivial.
The second contribution regards the transfer of the dynamic loads into a more detailed structural model of the aircraft, in order to study the stress distributions induced by the dynamic response. For this configuration, the structure was previously sized considering steady conditions, also for load factors larger than 1. Dynamic load conditions, however, might induce completely different stress states than the ones typically observed in the static sizing. Being this true also for conventional aircraft, for Box Wings, however, the situation is more involved due to the overconstrained nature of the system at the global level. As consequence of the external excitation (gust in this case) the two wings will have nonsynchronous dynamics, forcing eventually the joint to withstand large and unexplored stress states.

1.2 Overview of the Adopted Methodology

A 250-seat PrandtlPlane configuration is selected from the literature [6] [8]. The aeroelastic model of the chosen configuration is the typical "stick"-like one, well suited for aeroelastic analyses. More details on the configuration will be given in later sections. The aircraft is operating at its Maximum Take-off Weight with maximum payload configuration. Considered flight conditions are relative to the design cruise speed, V_c, at both sea level (h_{sl}) ad cruise altitude (h_{cr}).
According to the normative, gust parameters are selected and a list of gust gradient lengths is chosen to cover the specified interval. With the aid of the DYNRESP [12] code, extensively used in the aeroelastic certification phases of the A400M, discrete gust response of the aircraft is finally found.
Analyzing the time-response induced by the gusts, two dynamic load conditions that might show interesting/relevant stress states are selected. The loads are transferred to a more refined finite element model, better suited for stress analysis, which is carried out by commercial software MSC-Nastran. More details about the process can be found in [13].

2 THE PRANDTLPLANE 250

The box-wing aircraft under investigation is a 250-seat vehicle, whose artistic view is given in Figure 1. It is a mid-long range (6000 nm) design with a maximum take-off weight (MTOW) of 230 tons. The configuration was conceived in [13], which reports its properties and top-level details. Structural analyses were first carried out in [6] followed by aeroelastic investigations performed on a stick finite element model representation in [8]. Later on [7], a detailed finite element model was created to assess the stress distribution.
Studies regarding the aeroelastic behaviour of the configuration were continued in [9], [10] and [11]. This last effort considered the detailed finite element model, and added fuselage inertial effects in order to take into account the interaction between flight dynamics and structural modes. As it can be inferred by reviewing the vast body of literature on the topic [1], gust response on Box Wings has never been studied before.

2.1 Aeroelastic model

The aeroelastic model is composed of a stick-like description of the structure and has extra nodes to guarantee load/displacements transfer with the aerodynamic mesh, as it can be inferred from Figure 2.
The wing box is described by beam elements and the inertial effects of fuel and non structural systems are modelled through a combination of rigid elements and lumped masses. Details on this model can be found in reference [8].
To the wing finite element (FE) model, inertial effects have been added through concentrated masses and inertia points representing the fuselage, landing gear and engines. These inertial entities are rigidly connected to a node representing the location of the global CoG (in the undeformed case), which in turn is rigidly connected to the wing-fuselage intersection section, and to the fin root section, as shown in Figure 3.
Being the aerodynamic tool based on Doublet Lattice Method (DLM), the aerodynamic mesh representing the "mid-surface" is connected to the appropriate structural element for load and displacement transferring.

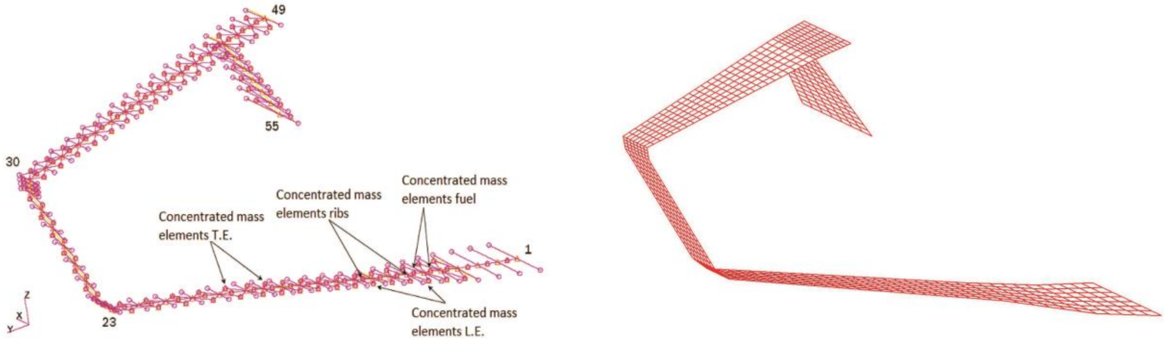

Figure 2: Structural model and aerodynamic mesh used for flutter analysis, rearranged from [8].

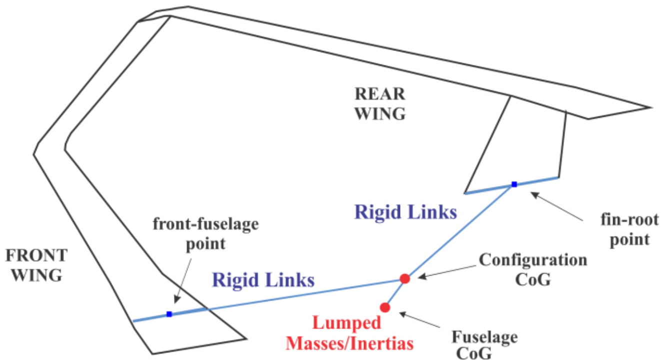

Figure 3: Conceptual model of the "free-flying" configuration.

2.2 Detailed structural FE model

The above model is well suited for dynamic aeroelastic analyses; however, if a stress analysis has to be carried out, a more refined structural representation is needed. To this aim, it is chosen to use the model developed in [7] because of its detailed description of the wing structure. It should be noted that this model was locally optimized in order to lighten the structure, with only static aeroelastic constraints in mind (steady limit load condition); however, the small local modifications are not considered to change dramatically the dynamic aeroelastic response. Thus, consistency between the stick and detailed model is retained.
The detailed FE model is shown in Figure 4, while the reader is referred to [7] for details.

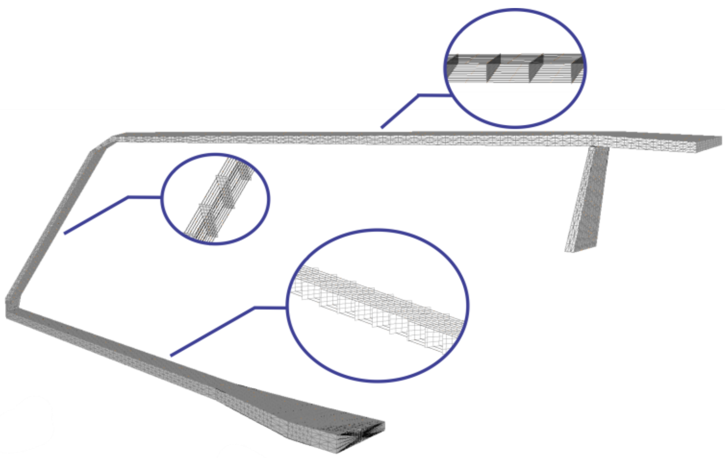

Figure 4: Detailed structural finite element model; rearranged from [11].

2.3 Flight envelope

As mentioned above, the design cruise speed V_c condition is considered, at two altitudes: cruise and sea level. At cruise altitude, h_{cr}=10500 m, the aircraft is designed to fly at M=0.85, relative to 253 m/s TAS (142 m/s EAS).
Following the regulations, and considering a transition altitude (dividing the region at constant Mach from the one at constant EAS) of h_{tr}=20000 fts, the sea level design cruise speed is approximately 196 m/s (M=0.58).
In all cases, the considered configuration is the maximum take-off weight (MTOW) one.

3 ATMOSPHERIC TURBULENCE AND DISCRETE GUST

It is well known that the atmosphere is essentially a turbulent media. Thus, since the outsets of modern aeronautics, efforts were carried out to better understand and model this "randomic" behaviour to design aircraft against its effect with a higher confidence level.
After several campaigns for collecting flight data, measurements were analyzed by means of statistical tools, based either on discrete (discrete gust) or continuous (continuous turbulence) events. Consequently, airworthiness regulations were shaped based on these approaches [15]. The interested reader is referred to [16] for a comprehensive review and in-depth information about the topic.
In this investigation, only the case of discrete symmetric gust is considered, leaving the study of response to antisymmetric and/or continuous turbulence for future research.

3.1 Discrete gust and Regulations

In the Discrete Gust case, an encountering of a gust velocity normal to the aircraft velocity is considered. Typically, the so-called *1-cosine gust* shape is chosen, see Figure 5. The response of the aircraft (considered as free in the air and flexible, and taking into account the unsteadiness of the aerodynamics) is then studied, for a set of gust lengths (Discrete Tuned Gust) as specified in the regulations.
An aircraft in the same weight class of the here considered Box Wing, i.e., a "large airplane", must comply with the certification specifications CS-25 of the European Aviation Safety Agency (EASA), when European normative is selected. Summarizing, the aircraft structure needs to support the limit loads induced by gust without detrimental permanent deformations. The procedure to obtain these limit load conditions is elucidated in section CS 25.341(a) (for the case of discrete gust).

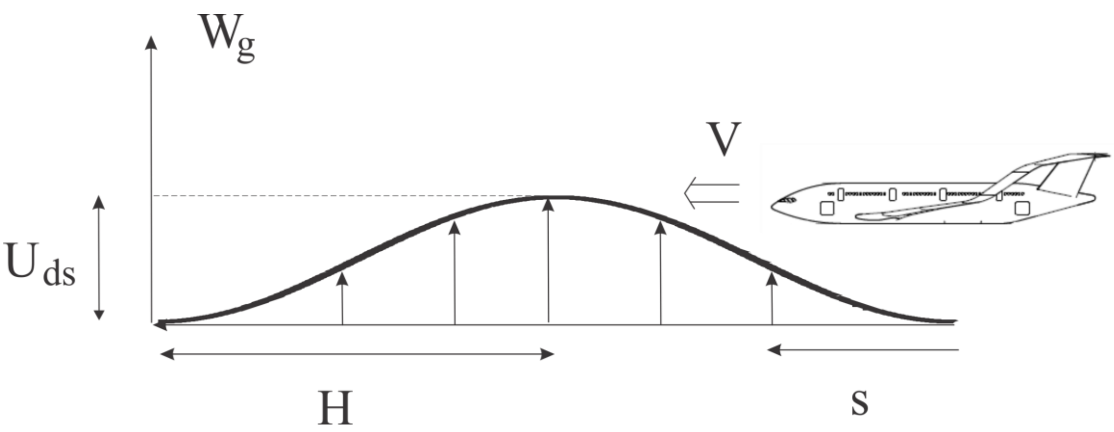

Figure 5: *1-cosine* gust shape, with characteristic gust velocities and dimensions, as specified in the CS 23.341(a)(2).

The shape of the gust is described by the following formula:

$$W_g = \frac{U_{ds}}{2}\left[1 - \cos\left(\frac{\pi s}{H}\right)\right]$$

being U_{ds} expressed as:

$$U_{ds} = U_{ref} F_g \left(\frac{H}{350}\right)^{1/6}$$

where U_{ref} depends on the flight altitude, and F_g is to be calculated as indicated in the regulations. An appropriate number of gust gradients H should be considered between the prescribed range $H = 9 \div 107\ m$ in order to detect the most critical response for each load quantity.

3.2 Considered gust parameters

Applying the above regulations to the considered points within the Box Wing flight envelope, and choosing 8 gust gradients, the following combination of design gust velocities are found:

Table 1: Gust parameters

V_c EAS [m/s]		U_{ref} EAS [m/s]		F_g		H [m]	U_{ds} EAS [m/s]	
h_{sl}	h_{cr}	h_{sl}	h_{cr}	h_{sl}	h_{cr}		h_{sl}	h_{cr}
196.1	142.3	17.21	10.36	0.74	0.96	9	8.44	6.58
						24	9.93	7.75
						39	10.77	8.40
						54	11.37	8.87
						69	11.85	9.24
						84	12.24	9.54
						99	12.58	9.81
						107	12.74	9.94

4 METHODOLOGY AND COMPUTATIONAL TOOLS

4.1 DYNRESP

DYNRESP is a powerful aeroelastic code that covers all aspects of aircraft dynamic loads. In fact, its features and methodology were based on needs and lessons learned during the A400M design process [12] [17]. The formulation is based on linear second-order frequency-domain equations of motion in generalized coordinates, which in case of open-loop gust response, reads:

$$\left[-\omega^2[M_{hh}] + i\omega[B_{hh}] + [K_{hh}] + q_\infty[Q_{hh}(i\omega)]\right]\{\xi(i\omega)\} = -q_\infty\left\{Q_{hg}(i\omega)\right\}\frac{w_G(i\omega)}{V} \qquad \textbf{(1)}$$

where $[Q_{hh}(i\omega)]$ are relative to modal displacements $\{\xi(i\omega)\}$; the right-hand-side term expresses the generalized aerodynamic forces due to a single sinusoidal gust velocity of amplitude $w_G(i\omega)$.
The left hand side matrices are usually obtained by means of external sources (ZAERO, NASTRAN).
Solution of the above equation,$\{\xi(i\omega)\}$, is then transformed back to the time domain (through Inverse-Fourier transform) giving $\{\xi(t)\}$, $\{\dot{\xi}(t)\}$ and $\{\ddot{\xi}(t)\}$.
Advanced strategies are employed to deal with singularities relative to rigid-body modes [17]. Several advanced features offered by DYNRESP and used in this investigation are, for the sake of brevity, not reported in this paper; details can be found in [17].
As outlined above, structural and aerodynamic data matrices are preliminary needed to run DYNRESP. Being the inherited aeroelastic model of the PrandtlPlane already set up in Nastran format, the authors relied on the DMAP capabilities to extract the sought data from Nastran and convert it into compatible DYNRESP format.

4.2 Analysis work-flow

The overall analysis flow has been characterized by the following steps.

NASTRAN Analysis set up and Data Extraction

In this initial step the aero-structural FE model needs to be augmented with information regarding flight conditions. Moreover, the appropriate number of normal modes and cut-off frequency, and the set of reduced frequency have to be chosen. This selection requires physical judgment and convergence analysis, as it is not trivial. The analysis file has to include the DMAP commands to extract the information needed by DYNRESP.

DYNRESP simulation

The input file for DYNRESP run needs then to be prepared. Particular care has to be spent for several aspects, as the selection of the IFFT time spacing for the output (which needs to be consistent with the cut-off frequency chosen above), the time interval, etc.

DYNRESP results post-processing and load transfer

The structural/internal forces can be easily retrieved if the stiffness matrix at finite element level is known, and equals (the equality is true only if no truncation of number of modes is performed, otherwise the equation holds only approximately) the dynamic unbalance:

$$[K][\phi]\,\{\xi(t)\} = -[M][\phi]\left\{\ddot{\xi}(t)\right\} - [B][\phi]\left\{\dot{\xi}(t)\right\} - \{F_A(t)\} \qquad \textbf{(2)}$$

where the last term represents the aerodynamic forces at the finite element nodes.

Stress analysis

The independent nodes where the internal forces are found coincide with the position of the ribs, where concentrated forces are introduced in the detailed FE model. Thus, the load transfer process is straightforward. Gust loads need to be superimposed to the cruise loads, which are extrapolated from the original model [7], thought for a steady limit load $n_z = 2.5$ condition, scaling down the steady loads to reach the condition $n_z = 1$. This process is a first approximation, as the aerodynamic loads need to be recalculated for the new trimmed configuration.

5 DISCRETE TUNED GUST RESPONSE OF THE BOX WING

In this section, the aeroelastic response of the stick FE model of the Box Wing is studied. As already stated above, only the aircraft in its Maximum Take-off Weight with Maximum Payload (MTOW-MP) is considered, flying at the design cruise speed, both at nominal cruise altitude and sea level.

5.1 Gust response, nominal cruise altitude

The operative conditions are the ones referring to V_c (M=0.85) at the cruise nominal height (10.500 meters). The 8 tabulated (see Table 1) gust gradient lengths are selected, and the response is studied. In Figure 6 the evolution in time of vertical displacement of the CoG, and the rotation of the longitudinal principal axis are plotted; in Figure 7 the generalized displacement evolutions are plotted for the first three elastic modes. As intuition suggests, largest displacements and rotations are relative to the largest gust gradient. For all cases an initial global pitching up motion, due to the increased effective angle of attack of the front wing, which first encounters the gust, is then reversed when the gust transverses also the rear wing. This pitching dynamics reversal happens before the aircraft CoG has reached its maximum displacement (*tmaxCoG*). Observing the evolution of the three elastic modes, the dynamics is slightly different between them.
For the first elastic modes (synchronous downward bending of the wings, see [8]), a cycle is observed within *tmaxCoG*. The second peak, relative to a downward deflection, is the largest.
The second elastic mode is characterized by tilting of the lateral joint along the longitudinal direction, i.e., a rotation along the span. Its evolution in time is faster than the one of the first elastic mode, and within *tmaxCoG*, approximately one and a half cycles have been developed.
The third elastic mode is characterized by an (almost) rigid translation and inward/outward tilting of the joint.

For the rigid and the first elastic mode, the gust gradient length postpones the peaks and increases the amplitude; this is not strictly true, however, for the second and third elastic modes. For example, the third elastic mode seems to be best triggered by an intermediate gust gradient length.

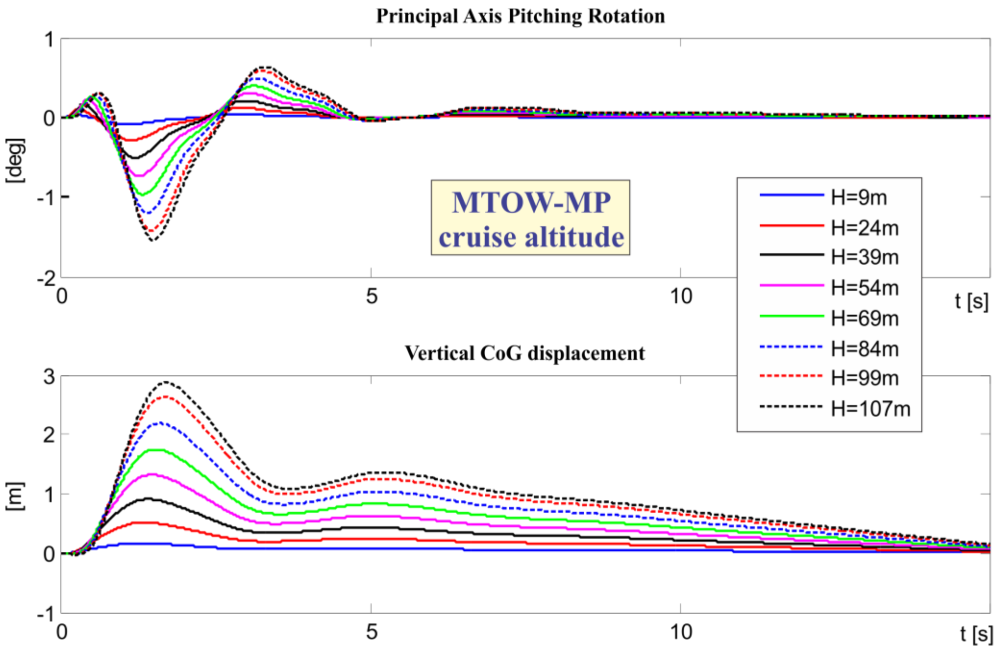

Figure 6: Gust response at cruise height. Vertical CoG displacement and rotation of the longitudinal principal axis.

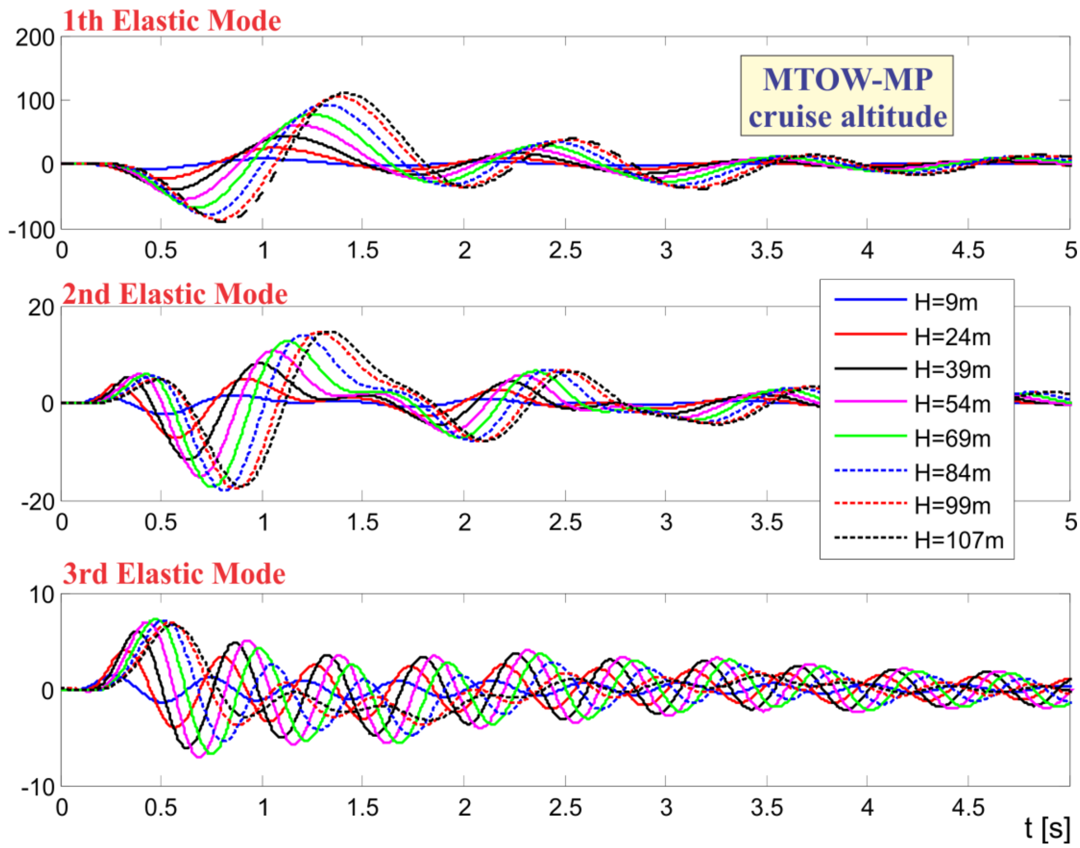

Figure 7 : Gust response at cruise level. (Elastic) modal displacements vs. time.

5.1 Gust Response, sea level

At sea level the design cruising speed V_c is approximately 191 m/s. Displacement responses are given in Figure 8 and Figure 9.

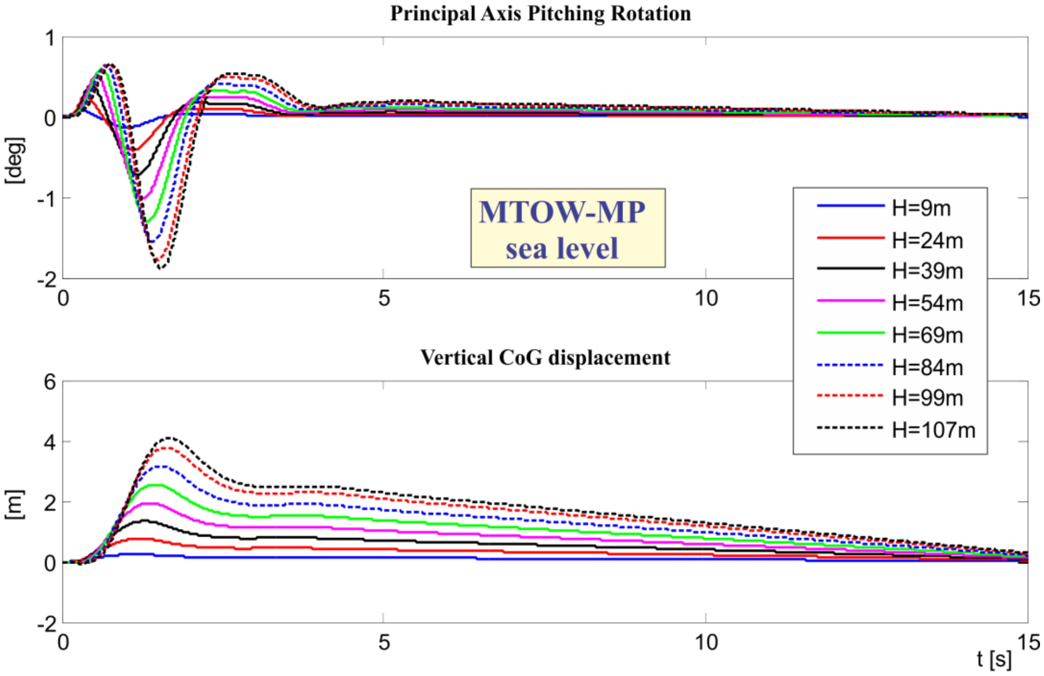

Figure 8: Gust response at sea level. Vertical CoG displacement and rotation of the longitudinal principal axis

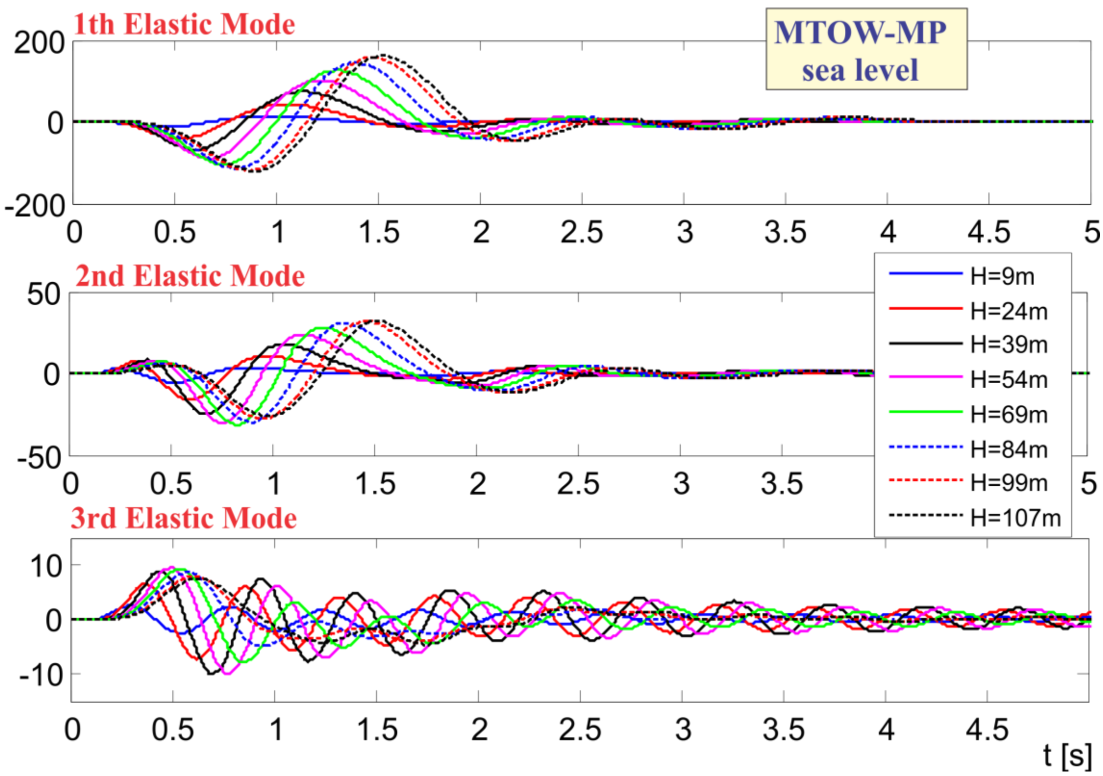

Figure 9: Gust response at sea level. (Elastic) modal displacements vs. time.

Similar trends as with the cruise altitude case are observed; it is noticed that both the rigid and the elastic modal displacements are larger.
In Figure 10 the sequence of the deformations induced by the gust is shown, for a small time interval of interest. It can be clearly seen how the gust-induced lift deforms the wings (flap-up) and moves the whole aircraft upward. During this motion, at some point the flapping motion is reversed (flap-down) although the configuration is still moving upward.
As a remark, to have the real deformed shapes, the displacements induced by the gust need to be superimposed to the ones relative to the trim condition.

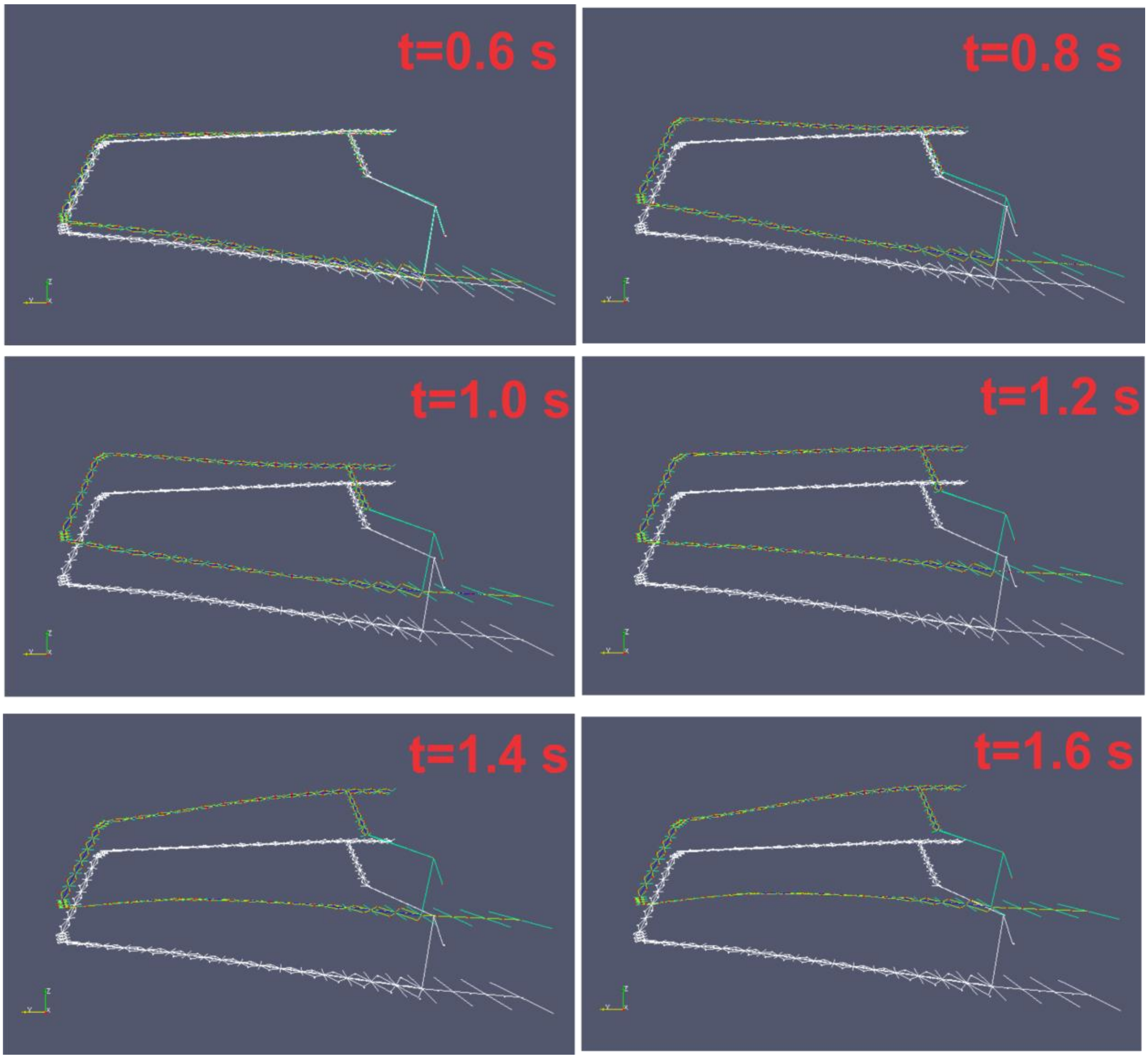

Figure 10: Snapshots taken from the gust response at sea level.

5.2 Load factor and aerodynamic forces

For both sea level and nominal cruise altitude cases, the largest rigid displacements are relative to the largest gust gradient length. Moreover, as shown in Figure 11, the largest vertical (incremental[1]) load factor is found, for both sea level and cruise altitude cases, to correspond to the largest gust gradient.

[1] *incremental* refers to increments in respect to the trim steady condition, for which $n_z = 1$.

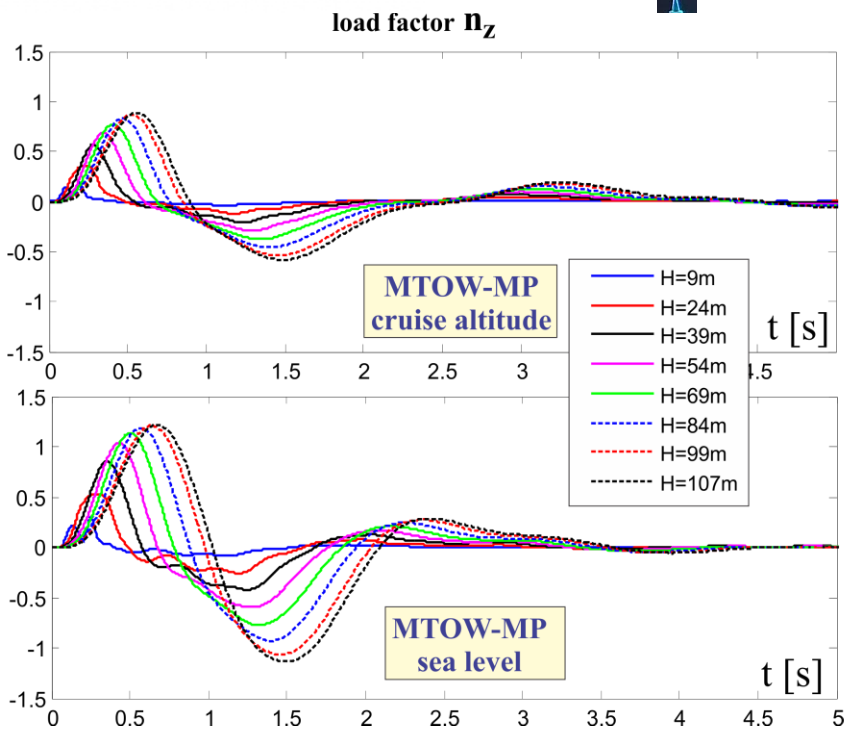

Figure 11: Incremental vertical load factor developed during gust response at cruise altitude and sea level.

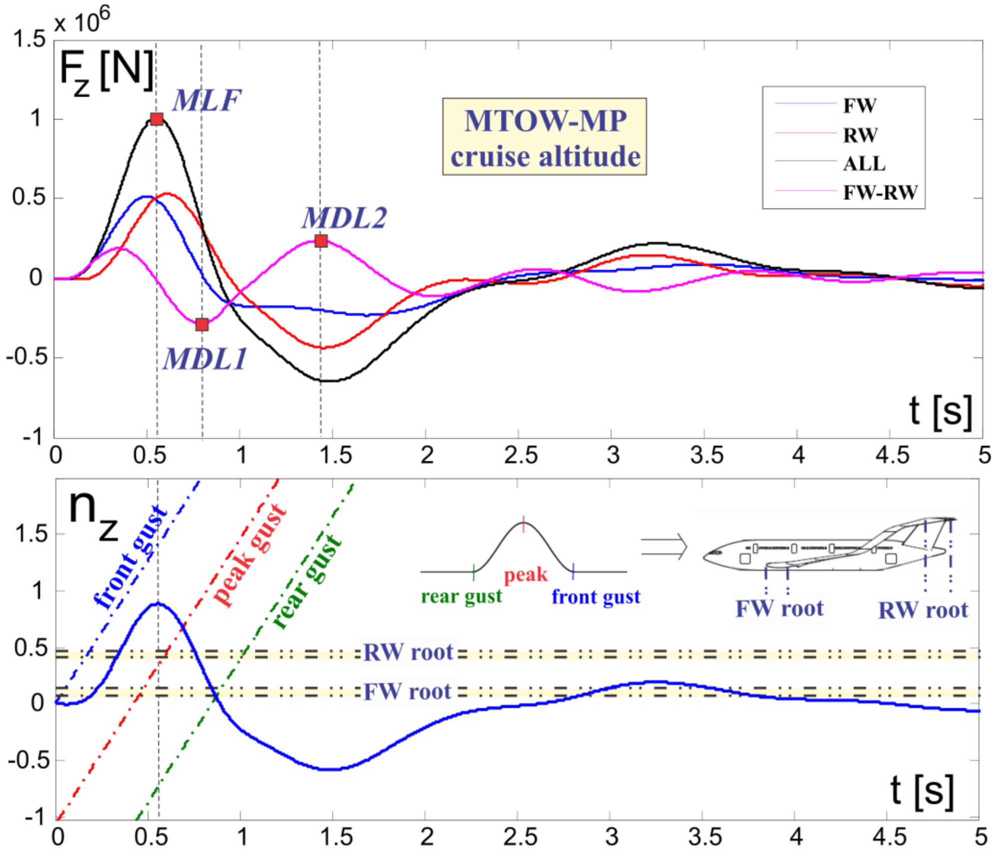

Figure 12: Gust response at cruise altitude. Above: incremental aerodynamic vertical forces produced by the whole configuration (ALL), by the front (FW) and rear (RW) wings, and difference between FW and RW (FW-RW). Below: incremental load factor (blue continuous line) and relative aircraft-gust position in time.

It is interesting to observe, for the largest gust gradient case (H=107 meters), the evolution of the aerodynamic forces acting on the lifting system sub-parts (front wing, rear wing, vertical joint), as depicted in Figure 12 and Figure 13.
The maximum load factor (increment) is obviously coincident with the point where the maximum (incremental) lift is produced; this condition will be referred to as maximum *load factor* (MLF).
Due to the particular arrangement of the wings, MLF falls after/before the maximum lift condition for the front/rear wing is achieved. In this condition, the gust peak is almost in-between the two wing roots, as it can be inferred by the lower sub-graphs. Looking at the modal displacement graphs, the MLF is relative to a condition of small vertical translation, and far from maximum displacement of the first and second elastic modes, whereas the third elastic mode shows an almost maximal involvement.
Further relevant conditions are the ones relative to maximal lift differential between the wings, that will be referred to as *maximum/minimum delta lift* (*MDL)*.
It is worth to notice that *MDL1* corresponds to a small overall lift condition in which the front wing does not carry lift; moreover, it is close to the peak-value of the first and second elastic modes, with smallest participation of the third elastic mode. The vertical displacement is still far from its maximum.
MDL2 is almost coincident with the point of largest negative load factor. The aircraft is at its maximum vertical displacement, and the down-stroke motion at its maximum amplitude, as it can be also inferred by the relative maximum in the first elastic mode displacement graph.

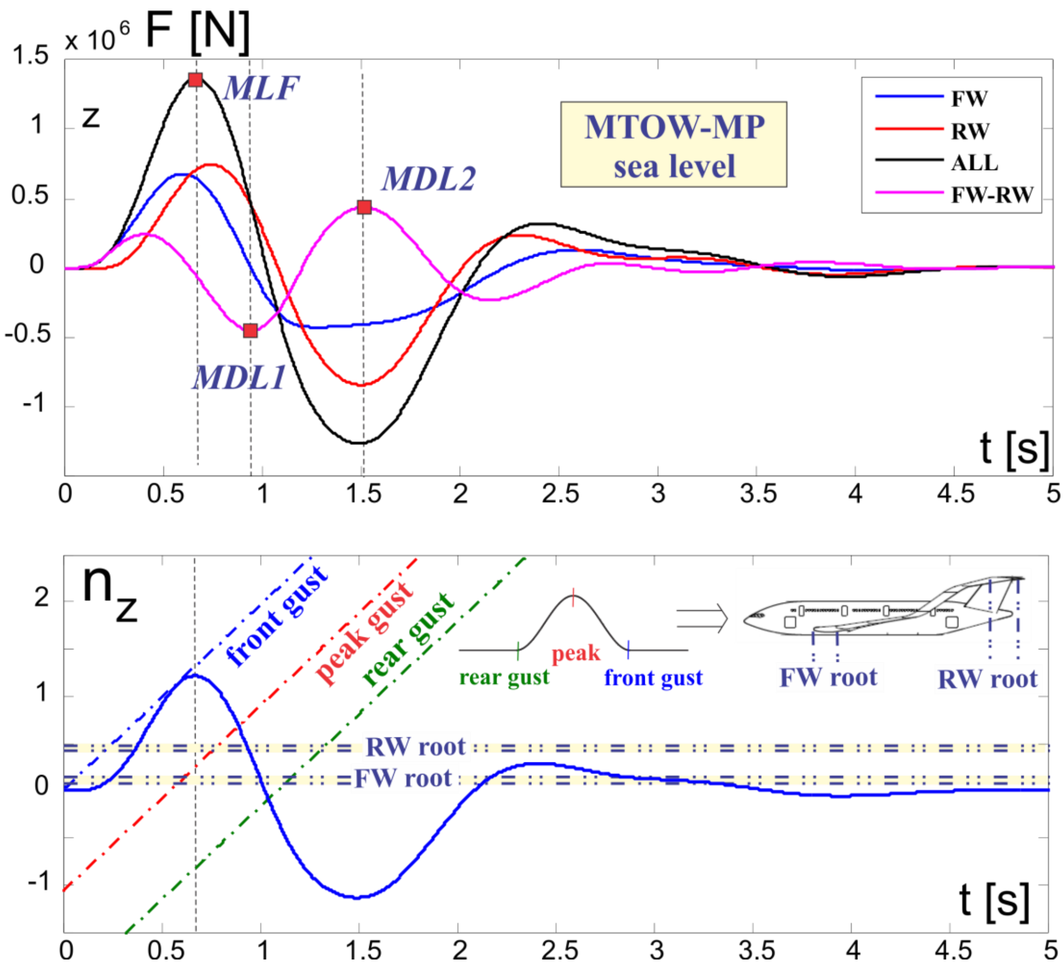

Figure 13: Gust response at sea altitude. Above: incremental aerodynamic vertical forces produced by the whole configuration (ALL), by the front (FW) and rear (RW) wings, and difference between FW and RW (FW-RW). Below: incremental load factor (blue continuous line) and relative aircraft-gust position in time

5.3 Remarks on the selection of dynamic loads for stress-check analysis

It is a formidable task to a-priori select the sizing load conditions for several components of the wings. This is generally true for traditional configurations, however, due to the overconstrained layout at the global level, is even more difficult for Box Wings.
The typical static sizing at limit load factor ($n_z = 2.5$), carried out for this model in [7], considered almost equally lifting wings. There are then analogies with the MLF conditions above, in terms of lift production. However, in dynamic responses, also inertial loads play an equally relevant role, thus, it is not correct to speculate on the criticality of one load condition based on the aerodynamic forces only.
In this preliminary investigation, a typical industrial certification-like approach, where thousands of analyses are needed, is not of interest, as the aim of this effort is to promote some general insight.
A possible option then, for selecting the critical load state is to observe the deformed shapes, and perform some speculations. With reference to Figure 10, the deformed shapes between 0.8 and 1 second, and between 1.4 and 1.6 seconds are of particular preliminary interest. The first one does share similarities with the static limit case. In the second deformed shape the wings present a distribution of curvature along the span which has inflexion points, consequence of different loads/moments transferred through the joint. For this reason, a completely distinct stress conditions is expected.

6 STRUCTURAL ANALYSIS

The internal structural forces, ideally equivalent to inertial, damping and aerodynamic forces, are evaluated as output of the dynamic response analysis on the stick model, on the beam nodes. These nodes correspond, in the detailed FE model, to rib locations, and are thus, points of introduction of loads. These forces are superimposed to the structural forces observed at ($n_z = 1$) trim condition, and stress analysis is then performed.
The three cases to be compared are:

a. load case relative to static limit load factor ($n_z = 2.5$), already analysed in [7].
b. load case relative to the response at sea level and largest gust gradient, time 0.9 s, superimposed to the load at trim ($n_z = 1$).
c. load case relative to the response at sea level and largest gust gradient, time 1.6 s, superimposed to the load at trim ($n_z = 1$).

The idea is to observe the general stress distribution and try to get some insight that can be of use for future dedicated and detailed stress analyses.

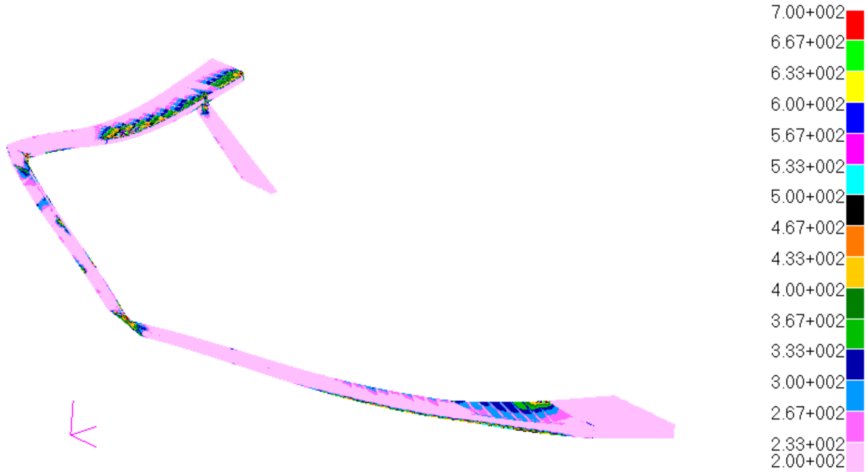

Figure 14: Stress state (Von Mises stress) for load condition (a).

6.1 Static limit load factor condition

In Figure 14 and Figure 15 stress analysis for case (a) is plotted. Results are identical to the ones reported in [7]. There are extensive are in which the stresses overcome the target design stress of 233 MPa for the used Aluminium. Some peaks are relative to the area of loads introduction, a finer design is locally needed. Other critical areas are the corners at the junctions. Some other areas are not fully stressed.

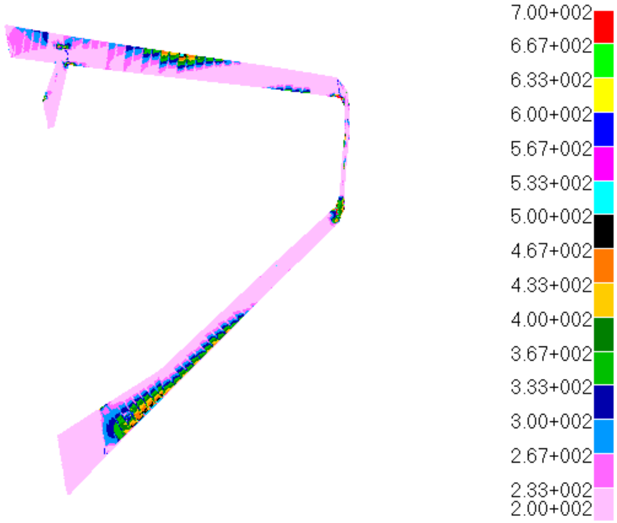

Figure 15: Stress state (Von Mises stress) for load condition (a). Bottom view.

6.2 Gust-induced loading condition (b)

For the sea level response at t=0.9 s, the maximum vertical deformation of the wing system is observed. The deformed shape is synchronous, and closely resembles the one of condition (a).
As a consequence, also stress states are comparable, as shown in Figure 16 and Figure 17. Actually, the upper region close to the front-wing kink experiences smaller stresses; on the contrary, the rear wing outboard trailing edge area is more critical.
For the lower panels on the front wing, now the region exceeding the admissible stress moves slightly outboard. Moreover, the inner region of the rear wing between the fins is more critically stressed.
A last remark concerns the fin structure, which seems to be subjected to larger stresses also far from the junction with the rear wing.

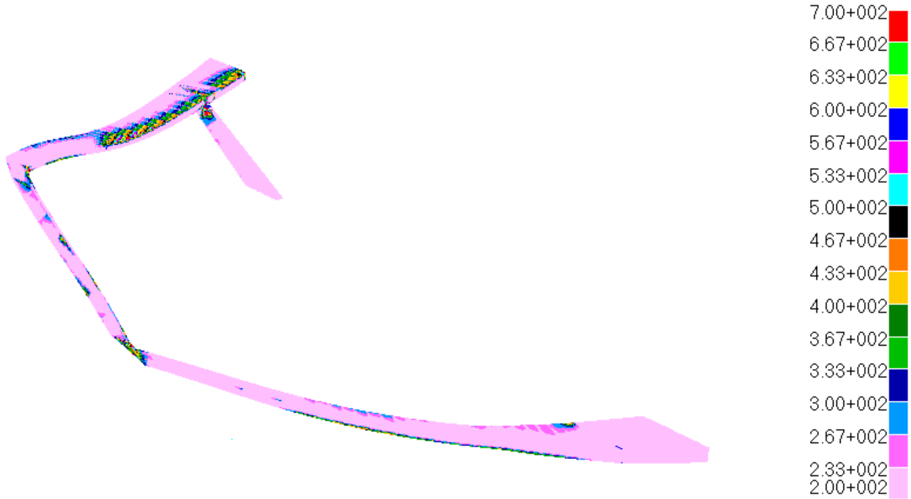

Figure 16: Stress state (Von Mises stress) for load condition (b).

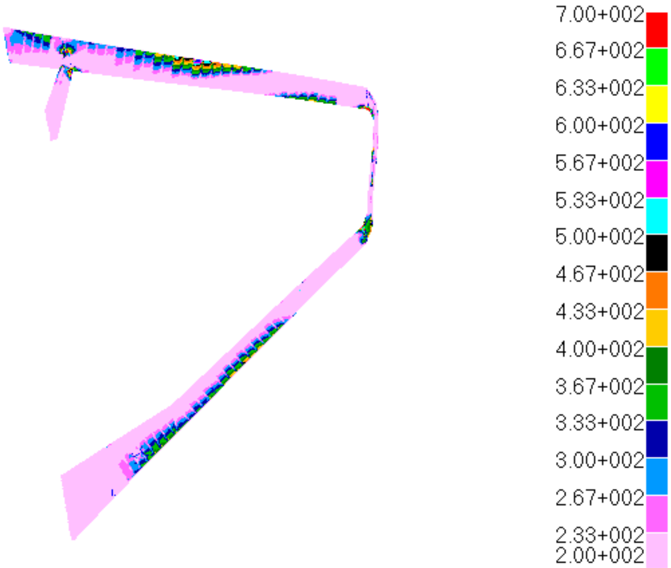

Figure 17: Stress state (Von Mises stress) for load condition (b). Bottom view.

6.3 Gust-induced loading condition (c)

For the sea level response at t=1.6 s, there is a deformed shape which is different than the ones studied in case (a) and (b).
The front wing has an emphasized downward bending whose pick is approximately at the midspan, as opposed to the previous upward bending having peaks at the wingtip. Moments and forces transmitted through the joint are thus different than the ones relative to the above loading conditions.
Stress analysis, however, suggests that stress-wise this load condition is generally well resisted by structure. The stress peaks are in fact extremely localized.

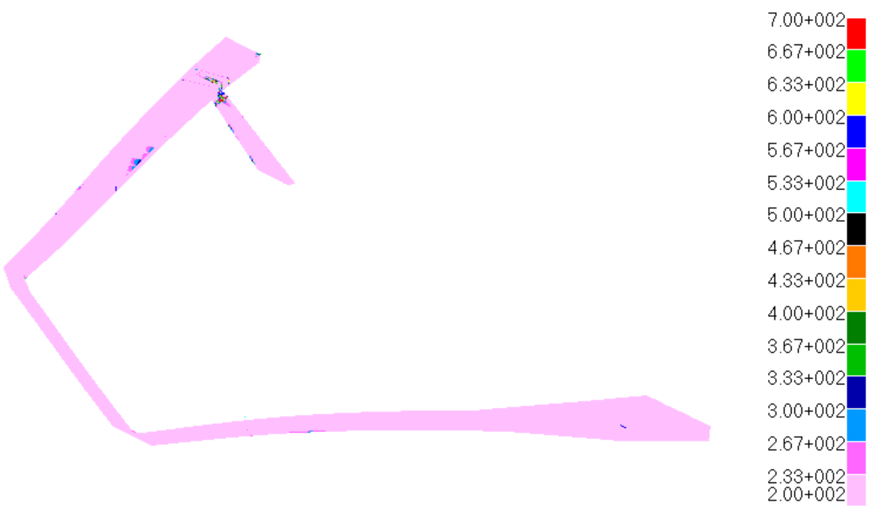

Figure 18: Stress state (Von Mises stress) for load condition (c).

7 CONCLUSIONS

A preliminary analysis on the symmetric discrete gust response of a Box Wings has been carried out for two points within the flight envelope, and one weight configuration (MTOW-MP).
The response with the largest deformations was relative to the sea-level condition with the largest gust gradient; load conditions relative to the dynamic response at two instants have been then selected, for a structural analysis.
In one condition, the deformed shape resembled the one typical of the static limit load ($n_z = 2.5$) condition. The stress analyses highlighted that some overstress areas shifted position, when compared to the limit load case.
In the second condition, the two wings presented smaller deflections, although the distribution of curvature highlights inflexion points. Stress analysis, however, suggested this state not to be critical stress-wise.

7.1 Future Work

The analyses only took into consideration the equivalent stress state. However, it is well known from the literature that one of the criticality of such configuration is the design of the lateral joint to avoid buckling occurrence. Thus, stress analyses might be augmented with a buckling one to have a more complete picture and insight into structural design of Box Wings.
A further interesting research step could be an optimization at detailed structural level against critical static and dynamic (gust induced) loads, followed by an evaluation of the weight penalties when only static or dynamic loads are considered.
In any case, stress or force/moments monitors need to be implemented to better detect the critical conditions.

8 AKNOWLEDGMENTS

The authors would like to thank Prof. Moti Karpel and his PhD student Federico Roizner at the Technion (Israel Institute of Technology) for their help and advices regarding DYNRESP code.

REFERENCES

[1] R. Cavallaro and L. Demasi, "Challenges, Ideas, and Innovations of Joined-Wing Configurations: A Concept from the Past, an Opportunity for the Future," *Progress in Aerospace Sciences ,* vol. 87, pp. 1-93, 2016.

[2] L. Prandtl, "Induced Drag of Multiplanes," 1924.

[3] R. H. Lange, J. F. Cahill, E. S. Bradley, R. R. Eudaily, C. M. Jenness and D. G. Macwilkinson, "Feasibility Study of the Transonic Biplane Concept for Transport Aircraft Applications," 1974.

[4] A. Frediani, V. Cipolla and E. Rizzo, "The PrandtlPlane Configuration: Overview on Possible Applications to Civil Aviation," in *Variational Analysis and Aerospace Engineering: Mathematical Challenges for Aerospace Design*, vol. 66, G. Buttazzo and A. Frediani, Eds., Springer US, 2012, pp. 179-210.

[5] A. Frediani, V. Cipolla and F. Oliviero, "IDINTOS the first prototype of an amphibious PrandtlPlane-shaped aircraft," *Aerotecnica & Missili Spazio, The Journal of Aerospace Science, Technology and Systems,* vol. 94, no. 3, pp. 100-114, January-July 2015.

[6] D. Dal Canto, A. Frediani, G. L. Ghiringhelli and M. Terraneo, "The Lifting System of a PrandtlPlane, Part 1: Design and Analysis of a Light Alloy Structural Solution," in *Variational Analysis and Aerospace Engineering: Mathematical Challenges for Aerospace Design*, vol. 66, G. Buttazzo and A. Frediani, Eds., Springer US, 2012, pp. 211-234.

[7] A. Frediani, F. Quattrone and F. Contini, "The Lifting System of a PrandtlPlane, Part 3: Structures Made in Composites," in *Variational Analysis and Aerospace Engineering: Mathematical*

Challenges for Aerospace Design, vol. 66, G. Buttazzo and A. Frediani, Eds., Springer US, 2012, pp. 269-288.

[8] N. Divoux and A. Frediani, "The Lifting System of a PrandtlPlane, Part 2: Preliminary Study on Flutter Characteristics," in *Variational Analysis and Aerospace Engineering: Mathematical Challenges for Aerospace Design*, vol. 66, G. Buttazzo and A. Frediani, Eds., Springer US, 2012, pp. 235-267.

[9] R. Cavallaro, R. Bombardieri, L. Demasi and A. Iannelli, "PrandtlPlane {J}oined {W}ing: Body Freedom Flutter, Limit Cycle Oscillation And Freeplay Studies," *Journal of Fluids and Structures,* vol. 59, pp. 57-84, November 2015.

[10] R. Bombardieri, R. Cavallaro and L. Demasi, "A Historical Perspective on the Aeroelasticity of Box Wings and PrandtlPlane with New Findings," 2016.

[11] R. Cavallaro, R. Bombardieri, S. Silvani, L. Demasi and G. Bernardini, "Aeroelasticity of the PrandtlPlane: Body Freedom Flutter, Freeplay and Limit Cycle Oscillation," in *Variational Analysis and Aerospace Engineering: Mathematical Challenges for Aerospace Design*, A. Frediani, Ed., Springer US, 2016.

[12] M. Karpel, A. Shousterman, C. Maderuelo, and H. Climent., "Dynamic Aeroservoelastic Response with Nonlinear Structural Elements," *AIAA Journal,* vol. Vol. 53, no. No. 11, pp. pp. 3233-3239, 2015.

[13] J. P. Santos, *Gust response of a box-wing aircraft,* Madrid: BS Thesis, 2017.

[14] A. Frediani, E. Rizzo, C. Bottoni, J. Scanu and G. Iezzi, "A 250 Passenger PrandtlPlane Transport Aircraft Preliminary Design," *Aerotecnica Missili e Spazio (AIDAA),* vol. 84, no. 4, pp. 152-163, 2005.

[15] J. C. J.R. Wright, Introduction to Aircraft Aeroelasticity and Loads, Wiley, 2015.

[16] F. Hoblit, Gust Loads on Aircraft: Concepts and Applications, Washington D.C: AIAA, 1988.

[17] M. Karpel, "Dynresp-10.1: Dynamic Response of Aircraft Structures to Gusts, Maneuver Commands and Direct Forces - Theoretical Manual," KARPEL Dynamic Consulting Ltd, TelAviv, Israel, 2016.

[18] A. S. Y. M. M. Karpel, "Rigid-Body Issues in FFT-Based Dynamic Loads Analysis," in *53rd AIAA/ASME/ASCE/AHS/ASC Structures, Structural Dynamics and Materials Conference*, Honolulu, Hawaii, 2012.